

# Measurement of anisotropic plasma properties along the magnetic nozzle expansion of an Electron Cyclotron Resonance Thruster

## IEPC-2017-437

*Presented at the 35th International Electric Propulsion Conference  
Georgia Institute of Technology • Atlanta, Georgia • USA  
October 8 – 12, 2017*

S. Correyero<sup>1</sup> J. Jarrige<sup>2</sup> D. Packan<sup>3</sup>  
*Office national d'études et de recherches aérospatiales (ONERA), Palaiseau, Paris, France*

and  
Eduardo Ahedo<sup>4</sup>  
*Universidad Carlos III Madrid, Leganes, 28911, Madrid, Spain*

**This work presents experimental measurements along the magnetized plume of the ECR thruster developed by ONERA. Langmuir probes are used to determine the electron energy probability function (eepf) at different axial positions, revealing the non-local character of the distributions. The second part of the paper details a combined diagnostics of non-intrusive diamagnetic loop measurements and laser induced fluorescence to estimate the perpendicular electron temperature inside the plasma source. Averaged perpendicular electron pressure, plasma density, ion velocity at the exit plane and perpendicular electron temperature are determined as functions of the mass flow rate.**

### Nomenclature

$V$	= induced voltage in the loop
$N_L$	= number of turns
$\Phi$	= magnetic flux
$B_z$	= total magnetic field in the axial direction
$B_{iz}$	= induced magnetic field in the axial direction
$B_{az}$	= applied magnetic field in the axial direction
$A$	= magnetic vector potential
$n_e$	= electron density
$P_{e\perp}$	= perpendicular electron pressure
$M$	= magnetization
$\gamma$	= flux
$u$	= mean velocity
$j$	= plasma currents
$r$	= radial coordinate
$\theta$	= azimuthal coordinate
$z$	= axial coordinate

---

<sup>1</sup> PhD student, Universidad Carlos III de Madrid (EP2 member), scorreye@ing.uc3m.es

<sup>2</sup> Research Scientist, Physics and Instrumentation Department, julien.jarrige@onera.fr

<sup>3</sup> Research Scientist, Physics and Instrumentation Department, denis.packan@onera.fr

<sup>4</sup> Professor, Equipo de Propulsion Espacial y Plasmas (EP2 director), eduardo.ahedo@uc3m.es

## I. Introduction

Among the cathodeless electric propulsion thrusters family, some of them such as the Electron Cyclotron Resonance Thruster [1, 2], the Helicon Thruster [3, 4] or the VASIMR [5] implement a magnetic nozzle at their final stage to accelerate and confine the plasma beam. Interest in magnetic nozzles has increased over the past decades, since they present multiple benefits for electric plasma thrusters, such as no wall losses during acceleration, no need for a neutralizer since the expanding beam is already quasineutral, possible magnetic thrust vectoring [6], etc. However, there are still some uncertainties concerning the physical mechanisms that guide the plasma beam throughout the magnetic nozzle expansion, such as the evolution of the electron distribution function, the trapped electrons, the ambipolar electric potential, the induced magnetic field effect, etc. Even though some authors have done significant research concerning magnetic nozzles during the past years [7 - 10], it is essential to provide experimental validation of the plasma behavior predicted by the theory.

Magnetic nozzles contain a divergent magnetic field created by a set of solenoids or permanent magnets where the plasma thermal energy is converted into axial kinetic energy. The ambipolar electric field developed throughout the expansion seems to be the main ion acceleration mechanism [11, 12]. This phenomenon has reopened outstanding problems, as for instance, the electron thermodynamics in a collisionless magnetized expansion. Electrons modelled as a Maxwellian population lead to infinite ion acceleration, since the ambipolar plasma potential remains unbounded. On another hand, Polytopic electron cooling laws need experimental validation and have demonstrated limited value. In this context, in order to obtain information about the electron energy distribution function along the expansion, this work presents Langmuir probe measurements throughout the magnetized expansion of an ECR thruster. Although the procedure to perform Langmuir probe measurements is well known [13, 14], the interpretation of the  $IV$  curve in magnetized anisotropic plasmas has still got high levels of uncertainty. For instance, taking into account the orientation and shape of the probe, as well as the sheath effect, become essential.

One of the main issues concerning electrostatic probe measurements is their intrusive character, since they operate extracting current from the plasma. Sometimes, while operating they can disturb significantly the thruster performance. This fact has a direct impact in the development of non-intrusive diagnostic techniques to determine plasma properties inside the plasma source and in the near-field. Among the non-intrusive diagnostics, we can find the diamagnetic loop, whose induced voltage at the thruster shutdown/ignition is proportional to the plasma perpendicular thermal energy. Concretely in the electron cyclotron resonance (ECR) thruster, plasma pressure is mainly due to electron pressure, since ion temperature is much lower than electron temperature  $T_i \ll T_e$ . For this device, the fact that diamagnetic currents only contribute to the perpendicular component of plasma pressure, makes it especially attractive as a directional diagnostic, since all the energy is initially stored in the perpendicular direction due to the cyclotron heating process. The diamagnetic loop measurement combined with other diagnostics to determine main plasma density can give rise to an estimate of the perpendicular electron temperature inside the plasma source [15, 16].

The paper is organized as follows: Section II introduces the ECR thruster and the two experimental set-ups carried out in this work: Langmuir probe measurements and diamagnetic loop combined with laser induced fluorescence. Section III presents the main results of the work and finally Section IV summarizes the conclusions and perspectives.

## II. Experimental set-up

### A. The ECR thruster: ONERA Facilities

Experiments are performed with two versions of the ECR thruster developed by ONERA [17] consisting of a coaxial plasma source of 1.85 and 27 mm diameter of the inner and outer conductors respectively, and a divergent magnetic field provided by a 130 A coil in version 1 and by a Neodymium permanent magnet in version 2. The source walls of the permanent magnet thruster are made of graphite, to reduce the effect of Eddy currents in the diamagnetic loop signal, and making feasible its calibration. The central magnetic field line of both thrusters is plotted in Figure 1 as a function of the axial distance to the backplate.

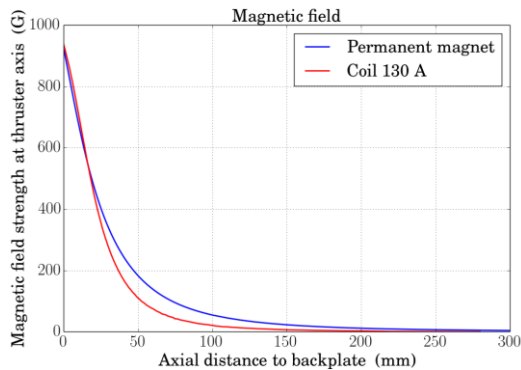


**Figure 1. Applied magnetic field strength at thruster axis in the permanent magnet and 130 A coil ECR thrusters.**

Palaiseau). Pumping is done with three turbomolecular pumps and one cryogenic pump, ensuring a base pressure in the chamber of  $3 \cdot 10^{-7}$  mbar.

## B. Diagnostics and operating conditions

The main goal of this work is to characterize the electron temperature throughout the ECR-magnetic nozzle in order to provide information related to the electron dynamics of a current-free magnetized expansion. For this task, two different set-ups are presented: Langmuir probe diagnostics to measure the electron energy probability function (EPPF) along the magnetic nozzle and diamagnetic loop combined with laser induced fluorescence (LIF) for determining the perpendicular electron temperature inside the thruster. Both set-ups are detailed below.

### B.1 Langmuir probe measurements

The EPPF along the magnetic nozzle of both versions of the ECR thruster (coil and permanent magnet) is determined using a Langmuir probe, consisting of a measurement tungsten wire of 0.1 mm diameter and 6 mm length, housed in a large 2 mm diameter ceramic tube. The probe was initially located on a rotational stage to orientate the measurement tip parallel or perpendicular to the magnetic field lines, but no difference between both measurements was found. The EPPF is directly determined from the second derivative of the measured  $IV$  curve.

The Langmuir probe is placed on a 200 mm translational stage so that its distance to the thruster exit plane varies from 55 mm to 255 mm. It was not possible to place the probe closer to 55 mm, since significant variations on the floating thruster potential were detected, an indication that the diagnostic was interfering the thruster performance. The floating potential is measured using a multimeter external to the vacuum chamber.

### B.2 Diamagnetic loop + LIF + current scans

An original diamagnetic loop setup has been designed to provide some measurement of the plasma magnetization. A 30 turns coil is placed around the thruster source walls, to provide an average value of the perpendicular electron thermal energy inside the ECR thruster. This is done by integrating the induced voltage during the thruster ignition/shutdown time window. The electron thermal energy is known to be converted into ion axial kinetic energy throughout the magnetic nozzle by means of the ambipolar electric potential. It is important to notice the global character of the measurement [18], since any significant change on the magnetic field near the loop would be recorded in the diamagnetic signal. This fact implies that magnetization of the magnetic nozzle must be considered to estimate properly the electron thermal energy inside the plasma source.

The main problem concerning the measurement of the diamagnetic loop is that plasma currents are not the only effect which can induce voltage in the loop. The signal is recorded when the thruster power is turned off, so there is a magnetic field variation due to the lack of plasma. This variation induces a voltage, whose integral in time is proportional to the number of loops satisfying Faraday's law:

$$V = -N_L \cdot \frac{\partial \Phi}{\partial t} \quad (1)$$

where  $N$  stands for number of loops,  $V$  for the induced voltage and  $\Phi$  magnetic flux through the coil.

However, any conductive material inside the region where the total magnetic field changes, such as the thruster walls or the vacuum vessel, would develop the well-known Eddy/Foucault induction currents [19]. Also, the ECR thruster of ONERA operates in a floating mode, so the walls charge to a voltage around 100-200 V, and discharge when the power is turned off. It was therefore necessary to simulate the discharge of the thruster with an external circuit without plasma to determine if there were any capacitive effects distorting the coil signal.

For the ECR thruster tested here,  $\Delta\Phi$  is only due to the magnetic field induced by the plasma before the shutdown, since the one induced by the permanent magnet does not vary with time. Plasma currents  $\mathbf{j}$  are responsible for the induced magnetic field, which is reflected in Ampere's equation:

$$\nabla^2 \mathbf{A} = -\mu_0 \mathbf{j} \quad (2)$$

where  $\mathbf{A}$  stands for the magnetic vector potential.

$$\mathbf{B}_i = \nabla \times \mathbf{A} \quad (3)$$

Since only the component of the magnetic field perpendicular to the loop surface would generate flux, the problem is reduced to the longitudinal induced field, which is caused by azimuthal plasma currents, the dominant currents in the plasma beam.

$$\mathbf{j} = j_\theta \mathbf{i}_\theta \quad (4)$$

$$\mathbf{A} = A_\theta \mathbf{i}_\theta \quad (5)$$

Therefore, the longitudinal component of Equation 3 in cylindrical coordinates remains:

$$B_{iz} = \frac{1}{r} \frac{\partial}{\partial r} (r A_\theta) \quad (6)$$

The magnetic flux due to plasma currents in sections of  $z = \text{const}$  can be expressed finally as:

$$\phi_i = \int \mathbf{B} \cdot \mathbf{n} dS = \int_0^R B_{iz} 2\pi r dr = 2\pi R A_\theta(R) \quad (7)$$

The computation of the magnetic potential vector requires knowing the distribution of plasma currents, as it is expressed in the Biot-Savart law, which in cylindrical coordinates takes the form of:

$$A_\theta(z, r) = \frac{\mu_0}{2} \iint d r' dz' \frac{r' j_\theta(z', r')}{\sqrt{(r - r')^2 + (z - z')^2}} \quad (8)$$

Equation 8 together with Equation 7 reveals the global integral character of the problem, where all plasma currents contribute to the computation of the induced magnetic flux that flows through the loop. Therefore, the problem relies in solving the azimuthal current distribution  $j_\theta(z', r')$  throughout the 2D magnetic nozzle expansion. The azimuthal current is related to the plasma pressure gradients through the electron momentum balance equation.

$$0 = -\nabla_\perp p_e - e n_e E_\perp + j_\theta B_z \quad (9)$$

Since the solving of the above 2D problem is challenging and no simple solution exists, we are forced to restrict the determination of the induced magnetic field and flow to order-of-magnitude estimates. In Equation 9,  $p_e$  represents electron pressure,  $n_e$  electron density and  $E$  the ambipolar electric field.  $B_z$  is the total magnetic field and  $\perp$  refers to the direction perpendicular to  $B$  in the meridian plane.

Concluding, the induced magnetic field can be estimated with Equations 3 and 6 as:

$$B_{iz} \sim \mu_0 j_\theta R \quad (12)$$

and the azimuthal currents  $j_\theta$  with Equation 11. Since the electric force is of the order of the pressure gradient [20], Equation 11 must be understood as an order of magnitude approach.

$$j_\theta \sim \frac{P_{e\perp}}{B_z R} \quad (11)$$

Therefore, if the total magnetic field is the order of the applied field, it is possible to relate approximately the magnetic flux that passes through the loop due to plasma currents with electron pressure as:

$$\phi_i \sim \frac{\mu_0 P_{e\perp} \pi R^2}{B_{az}} \quad (13)$$

Finally, to consider the finite shape of the plasma source and the consequent border effect in the magnetic flux lines measured by the loop, a shape factor calculated from a finite-element simulation in COMSOL is applied. The influence of the magnetic nozzle expansion in the diamagnetic loop signal has also been studied and taken into account. The simulation of magnetic flux lines measured by the loop is shown in Figure 2, where the 30 turns diamagnetic coil is located between the two outer blue lines, and the black rectangles stand for the thruster source walls. It is possible to estimate the percentage of negative flux measured by the loop, assuming magnetization is uniform inside the plasma source. Without any plume effect, the shape factor is around 36%. Since magnetization is due to the diamagnetic character of the plasma, it represents the perpendicular thermal pressure over the applied magnetic field. By applying flux conservation throughout the magnetic nozzle (Equation 15), an estimation of the plume magnetization order of magnitude can be done. Indeed, it can be appreciated from Equations 14 and 15 that magnetization should decrease at least as the inverse of the mean velocity. Actually, in reality, it would decrease even more, since perpendicular temperature also drops throughout the expansion.

$$M \sim \frac{P_{e\perp}}{B_{az}} = \frac{nT_{e\perp}}{B_{az}} \quad (14)$$

$$\Upsilon = \frac{nu}{B_{az}} = const \quad (15)$$

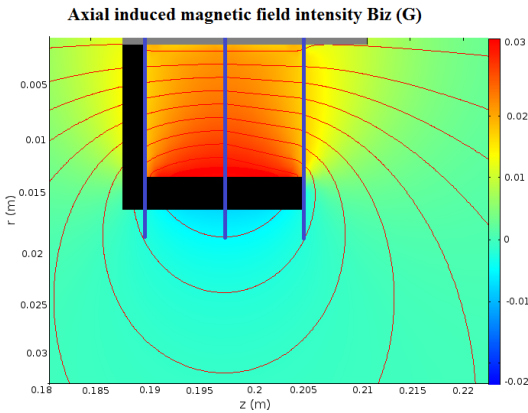


**Figure 2: Simulation of magnetic flux measured by the loop. The percentage of magnetic flux coming from the plasma source can be estimated by assuming uniform magnetization.**

Once the diamagnetic loop signal is validated, the electron perpendicular pressure inside the plasma source is determined at different operating conditions. The version used in this set-up was the permanent magnet ECR thruster, to avoid interferences of the diamagnetic loop with the own coil of the ECR coil thruster. The thruster is located on a 3-axis translational stage.

The diamagnetic loop measurement is combined with a Laser Induced Fluorescence diagnostic, detailed in [21], which determines the main ion axial velocity at the thruster exit plane. Finally, angular scans of ion current at 28 cm from the thruster exit allow determining the total current under the axisymmetric plume assumption. From the flux conservation law along the thruster

plume, the mean plasma density at the thruster exit plane can be estimated, and combined with the diamagnetic loop signal, the mean perpendicular electron temperature. It is important to notice that it is assumed that plasma density is uniform at the 15 mm plasma source, as well as the perpendicular electron temperature. Figure 3 shows a schematic of the set-up.

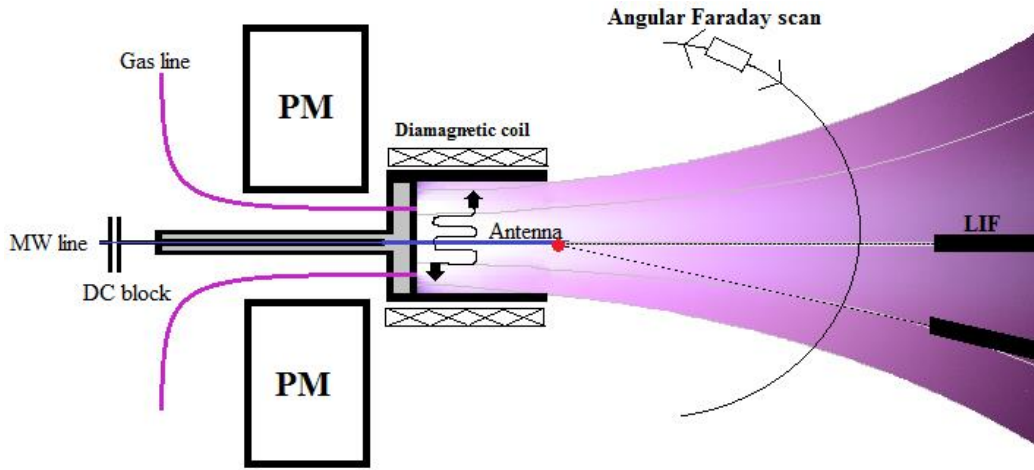


Figure 3: Schematic of the ECR thruster with the Diamagnetic coil + LIP + Faraday probe diagnostics.

### III. Results and discussion

#### A. Langmuir probes: Electron Energy Probability Function

The EEPF has been determined along the magnetic nozzle expansion as the second derivative of the  $IV$  Langmuir curve. The EEPF at different axial positions from the thruster exit is shown in Figure 4 (Fig.4 left corresponds to the coil ECR and Fig.4 right to the permanent magnet ECR). The horizontal axis in Figure 4 represents the electron kinetic energy, where plasma potential calculated from the inflexion point in the  $IV$  curve has been subtracted. The EEPF does not follow a Maxwellian distribution, which would look as a straight line in the logarithm scale. Differences between the EEPFs of both thrusters are mainly due to the magnetic field configuration.

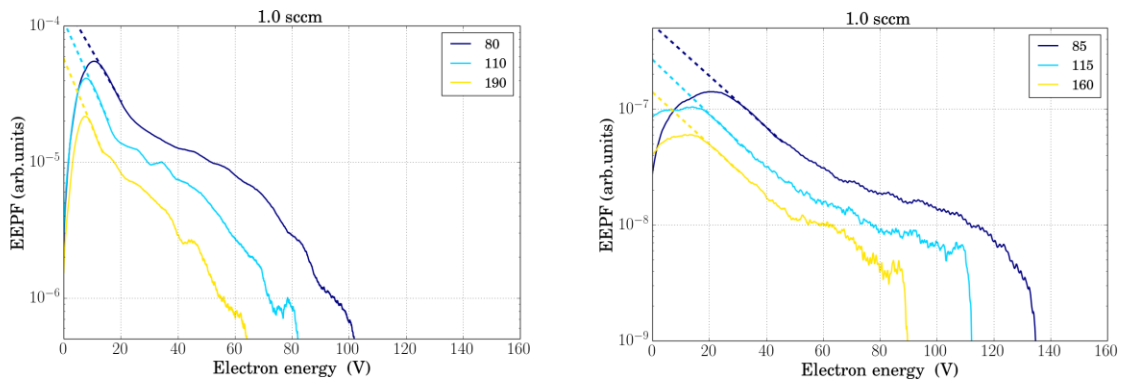


Figure 4: EEPF at three different axial positions at 30 W power and 0.1 mg/s. The legend indicates the distance to the thruster exit in mm. The left figure belongs to the coil ECR thruster and the right figure to the permanent magnet ECR.

In order to investigate the evolution of the EEPF along the magnetic nozzle expansion, the second derivative of the  $IV$  curve has been plotted against the bias voltage in Figure 5 at different axial positions. The low energy part has

been eliminated from the plot, since the signal is disturbed by probe resistance effects [22]. As well, the high energy part also presents uncertainty, which is mainly due to the decrease in the signal as a consequence of the density drop.

The EEPF can be estimated in a first approach by two Maxwellian distributions: High temperature low energy distribution, and low temperature high energy population. The fact that high energy electrons are colder than low energy electrons would be seen as a decrease in the main electron temperature along the expansion, since low energy electrons would be reflected back first as the ambipolar plasma potential drops. These results highlight the importance of considering the trapped electron population to study the non-kinetics of the electron dynamics of a magnetized collisionless expansion.

Furthermore, the EEPF maintains its shape at every axial position, only being depleted in low energies along the expansion. This result is consistent with previous work by Boswell et al [23], who found the same behavior in the magnetic nozzle of a helicon reactor.

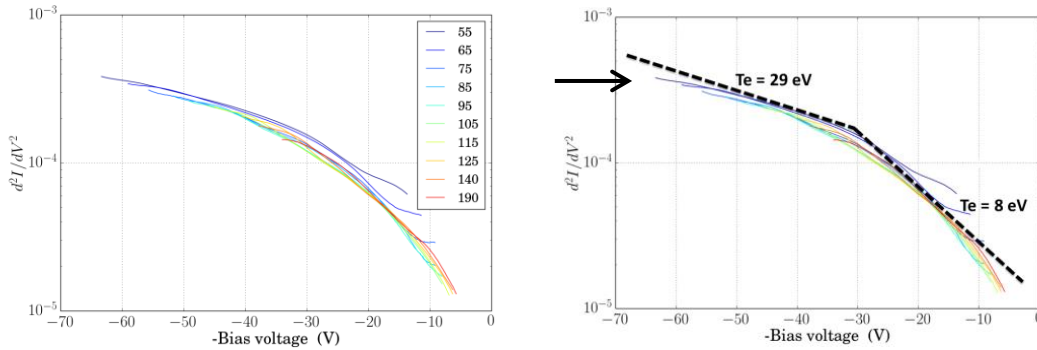


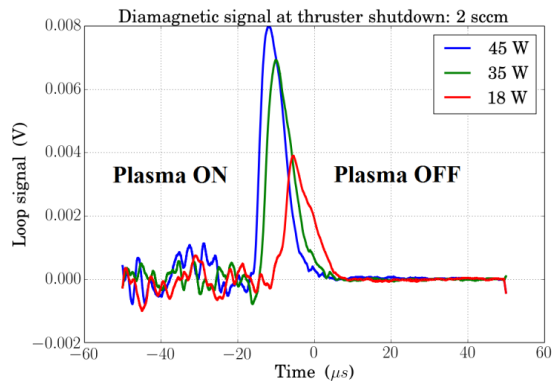
**Figure 5: Second derivate of the  $IV$  curve as a function of the bias voltage at different axial positions. The legend indicates the distance to the thruster exit in mm.**

## B. Non-intrusive diagnostics: Diamagnetic loop + LIF

It is essential to characterize plasma properties at the thruster exit and in the near field to be able to model the magnetic nozzle expansion. Langmuir curves can provide relevant information about the evolution of the EEPF along the magnetic nozzle. However, since current is collected from the magnetic nozzle plume, its performance can be significantly disturbed. In this work, it has not been possible to obtain information from Langmuir probes in the near field, and for this reason, we have developed a combination of non-intrusive diagnostics in order to estimate plasma properties at the thruster exit.

The electron perpendicular pressure is estimated by integrating the signal obtained from a diamagnetic loop wrapped around the thruster at the shutdown as it is detailed in Section II.B.2. The measurement is completed with LIF diagnostics to determine the mean ion velocity at the thruster exit, and angular scans of current to determine the total ion flux.

The combination of the three diagnostics provides an estimation of the perpendicular electron temperature at the plasma source.



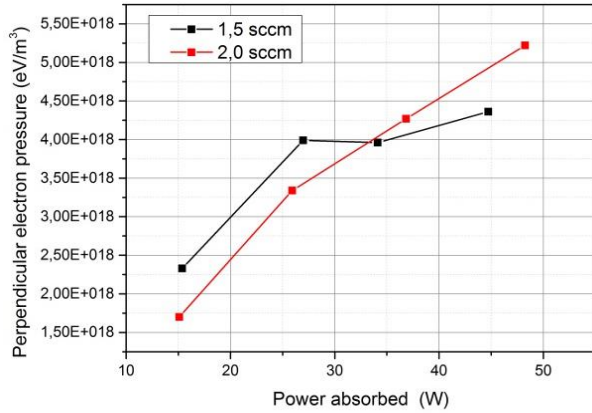
**Figure 6: Diamagnetic signal (V) with respect to time in the thruster shutdown for 2 sccm of Xenon, at different power levels (18 W, 35 W, and 45 W).**

Figure 6 shows three signals obtained for different powers with the 30 turns loop around the plasma source. The thruster shutdown lasts for 15  $\mu$ s, the time window where the main induced voltage of the loop is observed.

Other phenomena can be recorded with the diamagnetic signal: While the thruster is operating, oscillations in the induced field are detected by the loop, possibly coming from the plasma itself. Different oscillation frequencies are determined, and would be investigated in future work.

The thruster has been operated in different

conditions in order to investigate the effect of mass flow rate and power in the perpendicular electron pressure. Figure 7 shows the integrated signal, calibrated and corrected by the shape factor due to the finite shape of the thruster as a function of the absorbed power for two different mass flow rates (0.15 and 0.2 mg/s Xenon). As it can be observed, perpendicular electron pressure increases with the absorbed power. This is predicted by theory, since both density and perpendicular temperature increase with the power absorbed by the plasma.



**Figure 7: Perpendicular electron pressure of the plasma source measured by means of the diamagnetic loop as a function of the absorbed power for two different xenon mass flow rates.**

Plasma density at the thruster exit is estimated by performing angular scans of current at 28 cm with a Faraday gridded probe and identifying the mean ion velocity at the exit plane with a simple 1D laser induced fluorescence set-up. The ion mean axial velocity was determined and averaged at different locations of the thruster exit plane. Figure 8 shows the axial mean ion velocity as a function of the xenon mass flow rate measured by the LIF diagnostics. The mean ion velocity at the thruster exit decreases with the mass flow rate. This is directly related to the plasma potential developed at the plasma source.

Finally, the perpendicular electron temperature inside the plasma source is

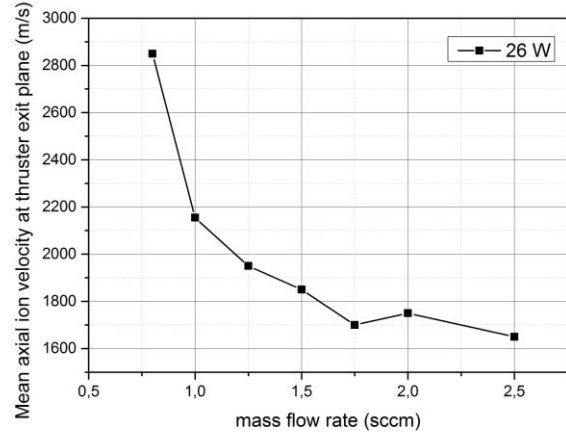
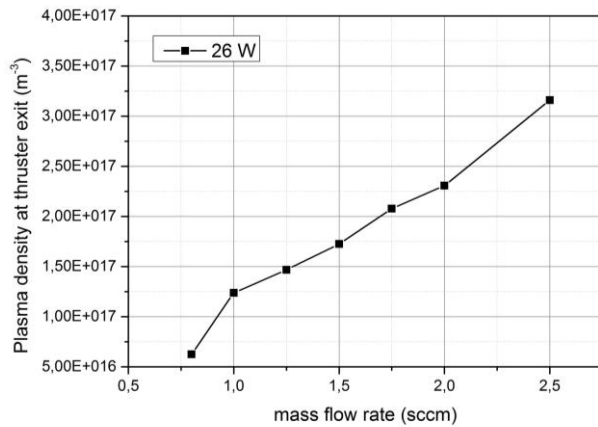


**Figure 8: Mean plasma density at the plasma source as a function of the mass flow rate, estimated combining angular scans of current and the mean axial ion velocity determined by LIF technique. 26 W were absorbed by the plasma.**

determined by combining the perpendicular electron pressure measurements and the mean plasma density. Figure 9 shows the variation of the mean perpendicular electron temperature with the mass flow rate. The fact that it decreases with mass flow rate is mainly due to the increase of collisions between electrons, which tends to thermalize the electron population and makes it more isotropic.

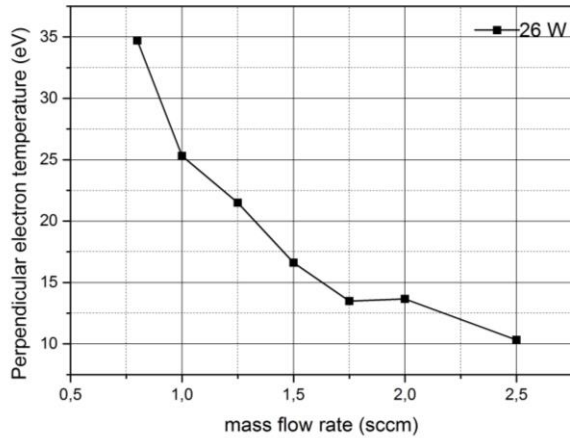


**Figure 9: Perpendicular electron temperature inside the plasma source as a function of xenon mass flow rate estimated by means of the diamagnetic loop and plasma density measurements. The thruster was operating at 26 W.**

## IV. Conclusions

This work presents several diagnostics in the magnetized plume of the ECR thruster developed by ONERA. First, Langmuir probes have been used to determine the  $IV$  curve at different axial positions. The EEPFs have been determined by performing the second derivative of this curve. Non-Maxwellian distributions have been found, but all the EEPFs seem to lie on the same curve, which is depleted throughout the expansion. The EEPFs can be approximated by two different contributions: a high temperature low energy distribution, and a low temperature high energy population.

The second part of this work presents an original combination of diagnostics of diamagnetic loop, laser induced Fluorescence, and angular scans of current. The primary aim was to determine the perpendicular electron temperature inside the plasma source. For this task, a diamagnetic loop was calibrated to determine the perpendicular electron pressure at the thruster shutdown. While the thruster was operating in a steady state, LIF was performed to determine the mean ion velocity at the thruster exit plane, where several points were analyzed and averaged. Finally, angular scans of current at 28 cm from the thruster exit determined the total ion current. By conservation of flux, the mean plasma density at the exit plane has been estimated, and together with the averaged perpendicular electron pressure measurements, the mean perpendicular electron temperature.

It is important to highlight the non-local character of the diamagnetic loop diagnostic, being essential to study the impact of surrounding plasma, such as the magnetized thruster plume. More accurate modelling of the thruster and the magnetic nozzle could improve the electron pressure estimate, reducing significantly the margin of error. Despite its non-locality character, the diamagnetic loop provides information about anisotropic properties, since it accounts only for the perpendicular plasma thermal energy. This directional measurement can provide insight of the physics involved in devices where anisotropic properties are relevant.

## Acknowledgments

This work was made in the framework of project MINOTOR that has received funding from the European Union's Horizon 2020 research and innovation programme under grant agreement No 730028.

## References

- <sup>1</sup>Jarrige, Julien, et al. "Characterization of a coaxial ECR plasma thruster." *44th AIAA Plasmadynamics and Lasers Conference*. 2013.
- <sup>2</sup>Sercel, Joel C., and Dennis J. Fitzgerald. "ECR plasma thruster research-Preliminary theory and experiments." *No. AIAA-Paper-89-2379; CONF-8907118--*. Monterey, CA (US); AIAA, 1989.
- <sup>3</sup>Pavarin, Daniele, et al. "Design of 50 W helicon plasma thruster." *31st Int. Electric Propulsion Conf., Ann Arbor, MI*. 2009.
- <sup>4</sup>Takahashi, Kazunori, et al. "Performance improvement of a permanent magnet helicon plasma thruster." *Journal of Physics D: Applied Physics* 46.35 (2013): 352001.
- <sup>5</sup>Diaz, Franklin R. Chang. "The VASIMR rocket." *Scientific American* 283.5 (2000): 90-97.
- <sup>6</sup>Merino, Mario, and Eduardo Ahedo. "Towards thrust vector control with a 3D steerable magnetic nozzle." *34th International Electric Propulsion Conference (Electric Rocket Propulsion Society, Fairview Park, OH, 2015)*. 2015.

- <sup>7</sup>Ahedo, E., and M. Merino. "Two-dimensional supersonic plasma acceleration in a magnetic nozzle." *Physics of Plasmas* 17.7 (2010): 073501.
- <sup>8</sup>Fruchtman, A., et al. "A magnetic nozzle calculation of the force on a plasma." *Physics of Plasmas* 19.3 (2012): 033507.
- <sup>9</sup>Arefiev, Alexey V., and Boris N. Breizman. "Magnetohydrodynamic scenario of plasma detachment in a magnetic nozzle." *Physics of Plasmas* 12.4 (2005): 043504.
- <sup>10</sup>Hooper, E. B. "Plasma detachment from a magnetic nozzle." *Journal of Propulsion and Power* 9.5 (1993): 757-763.
- <sup>11</sup>Arefiev, Alexey V., and Boris N. Breizman. "Ambipolar acceleration of ions in a magnetic nozzle." *Physics of Plasmas* 15.4 (2008): 042109.
- <sup>12</sup>Longmier, Benjamin W., et al. "Ambipolar ion acceleration in an expanding magnetic nozzle." *Plasma Sources Science and Technology* 20.1 (2011): 015007.
- <sup>13</sup>Lam, S. H. "Unified theory for the Langmuir probe in a collisionless plasma." *The Physics of Fluids* 8.1 (1965): 73-87.
- <sup>14</sup>Chen, Francis F. "Langmuir probe diagnostics." *IEEE-ICOPS Meeting, Jeju, Korea. Vol. 2. No. 6. 2003.*
- <sup>15</sup>Katsumata, Ryota, et al. "Temperature anisotropy measurement using diamagnetic loop array." *Japanese journal of applied physics* 31.7R (1992): 2249.
- <sup>16</sup>Tonetti, G., J. P. Christiansen, and L. De Kock. "Measurement of the energy content of the JET tokamak plasma with a diamagnetic loop." *Review of Scientific Instruments* 57.8 (1986): 2087-2089.
- <sup>17</sup>Cannat, F., et al. "Optimization of a coaxial electron cyclotron resonance plasma thruster with an analytical model." *Physics of Plasmas* 22.5 (2015): 053503.
- <sup>18</sup>Hutchinson, Ian H. "Principles of plasma diagnostics." *Plasma Physics and Controlled Fusion* 44.12 (2002): 2603.
- <sup>19</sup>Bottiglioni, F. (1970). "Influence of metallic walls on plasma diamagnetic measurements." *Plasma Physics*, 12(2), 131.
- <sup>20</sup>Merino, M., & Ahedo, E. (2016). "Effect of the plasma-induced magnetic field on a magnetic nozzle." *Plasma Sources Science and Technology*, 25(4), 045012.
- <sup>21</sup>Jarrige, J., et al. "35th Int. Electric Propulsion Conf., Atlanta, IEPC-2017-437"
- <sup>22</sup>Godyak, V. A., and V. I. Demidov. "Probe measurements of electron-energy distributions in plasmas: what can we measure and how can we achieve reliable results?." *Journal of Physics D: Applied Physics* 44.23 (2011): 233001.
- <sup>23</sup>Boswell, Rod W., et al. "Non-local electron energy probability function in a plasma expanding along a magnetic nozzle." *Frontiers in Physics* 3 (2015): 14.